

# The Internal Conversion Electron Spectrum of $^{147}\text{Nd}$

E. BASHANDY and A. ABD EL-HALIEH

Nuclear Physics, Department, Atomic Energy Establishment, Cairo, U. A. R.

(Z. Naturforschg. **22 a**, 154—164 [1967]; received 15 June 1966)

The internal conversion electron spectrum following the  $\beta$ -decay of  $^{147}\text{Nd}$  has been studied using an iron yoke and an iron free double focussing  $\beta$ -ray spectrometer at a momentum resolution of about 0.2%. A total of 66 transitions has been ascribed to this decay. On the basis of statistical analysis of sum relationships for the transition energies, combined with earlier reported coincidence results, a decay scheme involving 16 excited levels is suggested. The experimental data indicate a higher state at 763 keV. Its energy is close to the high state observed in other promethium nuclei.

The multipolarity assignment for each transition was obtained by comparing the observed conversion line intensity ratios with the theoretical line intensity ratios of SLIV and BAND. From the multipolarity values obtained, the spins and parities of the excited levels in  $^{147}\text{Pm}$  are assigned and discussed in terms of recent nuclear models.

The decay scheme of  $^{147}\text{Nd}$ , 11.1 days half-life, has been investigated by different authors<sup>1-7</sup>. As a result, energy levels in  $^{147}\text{Pm}$  at 91, 411, 532 and 690 keV directly fed by  $\beta$  decay of  $^{147}\text{Nd}$ , were introduced by HANS et al.<sup>1</sup> and were subsequently confirmed by several investigators<sup>7</sup>. The coincidence between 91 and 199 keV  $\gamma$  rays observed by CORK et al.<sup>2</sup> necessitated introduction of an energy level either at 289 keV or at 491 keV. EVANS<sup>3</sup> suggested an additional level at 230 keV to accommodate the  $\gamma$  rays of energy 230, 260 and 300 keV, reported originally by RUTLEDGE et al.<sup>4</sup>. WENDT and KLEINHEINZ<sup>5</sup> proposed an energy level at 182 keV, as formed by the new  $\beta$  group of end point energy 719 keV and of intensity  $\approx 10\%$  which was observed by them. Coincidence measurements have been carried out by GUNYE et al.<sup>6</sup> and SASTRY et al.<sup>7</sup>. Their results were in agreement and the constructed level scheme suggested<sup>7</sup> is quite different from that previously obtained, see Fig. 1. The mode of decay of the 723 keV level was observed to be by crossover transition and no cascades<sup>7</sup>. The spin and parity of the ground state of  $^{147}\text{Nd}$  has been measured by ABRAHAM<sup>8</sup> to be  $5/2^-$ . The ground state spin of  $^{147}\text{Pm}$  has also been determined<sup>9</sup> to be  $7/2$ . All the  $\beta^-$  transitions from the ground state of  $^{147}\text{Nd}$ , feeding the excited states of  $^{147}\text{Pm}$ , have been classified as

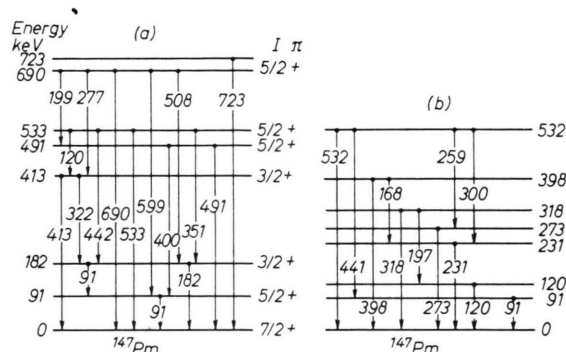


Fig. 1. Energy level diagram of  $^{147}\text{Pm}$ , (a) proposed by SASTRY et al.<sup>7</sup> and (b) by RUTLEDGE et al.<sup>4</sup>.

first forbidden with a spin change of zero or one and with a change of parity<sup>3,4</sup>. Thus, each excited level in  $^{147}\text{Pm}$  must have one of the following values  $3/2^+$ ,  $5/2^+$ ,  $7/2^+$ . For the energy level at 182 keV three possible spin values  $3/2^+$ ,  $5/2^+$  or  $7/2^+$  were suggested<sup>7</sup>. Though no definite conclusion in regard to the spin value of that level can be drawn from previous studies, the assignment  $3/2^+$  promised<sup>7</sup> to be more favourable. The  $\gamma$ - $\gamma$  directional correlation measurement in  $^{147}\text{Nd}$  assigned<sup>10</sup> the energy levels of  $^{147}\text{Pm}$  at ground state, 91 keV, 410 keV and 690 keV to be  $7/2^+$ ,  $7/2^+$ ,  $7/2^+$  and  $5/2^+$ , respectively.

<sup>1</sup> H. S. HANS, B. SARAF, and C. E. MANDEVILLE, Phys. Rev. **97**, 1267 [1955]; **98**, 1173 [1955].

<sup>2</sup> J. M. CORK, M. K. BRICE, R. G. HELMER, and R. M. WOODS, Phys. Rev. **110**, 526 [1958].

<sup>3</sup> P. R. EVANS, Phil. Mag. **3**, 1061 [1958].

<sup>4</sup> W. C. RUTLEDGE, J. M. CORK, and S. B. BURSON, Phys. Rev. **86**, 775 [1952].

<sup>5</sup> H. D. WENDT and P. KLEINHEINZ, Nucl. Phys. **20**, 169 [1960].

<sup>6</sup> R. GUNYE, R. JAMBUNATHAN, and B. SARAF, Phys. Rev. **122**, 172 [1961].

<sup>7</sup> V. V. G. SASTRY, V. LAKSHMINARAYANA, and SWAMI JNANANANDA, Indian J. Pure Appl. Phys. **2**, 307 [1964].

<sup>8</sup> K. M. ABRAHAM, Phys. Rev. **103**, 54 [1957].

<sup>9</sup> P. F. A. KLINKENDERG and F. S. TOMPKINS, Physica **26**, 103 [1960].

<sup>10</sup> A. R. ARYA, Phys. Rev. **122**, 1226 [1961].



In view of the inconclusive nature of the results mentioned above, it was considered that further investigations of this isotope, employing high resolution double focussing  $\beta$ -ray spectrometers are of great interest and may yield useful information regarding the properties of various energy levels and the cascade modes of decay.

The study of the excited states of  $^{147}\text{Pm}$  is essential for a better understanding of the energy level systematics in this region of isotopes. The present investigation was accordingly undertaken in order to search for further low intensity transitions in the decay of  $^{147}\text{Nd}$  and to obtain information which could permit a comparison with recent nuclear theories.

## 1. Experimental Procedure

### 1.1 Source preparation

The samples were prepared by irradiating  $\text{Nd}_2\text{O}_3$ , with the Nd electromagnetically enriched to  $\sim 99\%$   $^{146}\text{Nd}$ , in Dido reactor at Harwell for a period of 23 days in a flux of about  $10^{14}$  neutrons/cm $^2$ ·s. The inactive material was deposited onto an aluminium foil to thickness 0.7 mg/cm $^2$  using a cathodic sputtering technique. The  $\text{Nd}_2\text{O}_3$  was sputtered uniformly on the aluminium using a special mask. The thickness of the material deposited was estimated to be  $\sim 80$   $\mu\text{g}/\text{cm}^2$  and of dimension  $1.5 \times 0.2$  cm $^2$ .

Because of the simultaneous production of  $^{149}\text{Nd}$  ( $T_{1/2}=1.8$  hr) and its daughter  $^{149}\text{Pm}$  ( $T_{1/2}=50$  hr) which may be present, irradiated samples were allowed to decay for enough time to get rid of these shortlived activities if they exist.

### 1.2 Apparatus

The excited levels in  $^{147}\text{Pm}$  were studied from the decay of the (11.1 d)  $^{147}\text{Nd}$ . Energies and relative intensities of the conversion electron lines were measured by means of two double focussing  $\beta$ -ray spectrometers, and iron yoke instrument\* ( $\varrho_0=22.5$  cm) and an iron free double focussing  $\beta$ -ray spectrometer ( $\varrho_0=50$  cm) constructed in our laboratory. With the latter instrument, relative momentum measurements could be made with an accuracy of a few parts in  $10^5$ . In most of the investigations described here, a resolution in momentum of  $\sim 0.2\%$  was used. It was not practical to operate at better resolution due to the low specific of the source. Fortunately, improved resolution was not required to resolve any closely spaced line groups. The detectors in both spectrometers were GEIGER-MÜLLER tubes with end window of  $1.6-1.8$  mg/cm $^2$  mica.

### 1.3 Conversion electron measurements

The study of the  $^{147}\text{Nd}$  decay was initiated by scanning the conversion electron spectrum in the energy range 40–760 keV. The measurement was followed up in a repetitive way to scan: 1) the various line groups observed in the survey, 2) line groups previously reported and 3) line groups predicted by our proposed decay scheme. In some of these latter studies improved counting statistics were obtained. A total of 135 conversion lines were found. The decay of the lines was followed by taking records repeatedly. No line with a half-life which could not be ascribed to the decay of  $^{147}\text{Nd}$  was observed.

To provide a reference line for the energy measurements on  $^{147}\text{Nd}$  decay, the conversion lines of the 84 keV transition in  $^{170}\text{Yb}$ , the 412 keV transition in  $^{198}\text{Hg}$  and the 661 keV transition in  $^{137}\text{Ba}$  were carefully measured on an absolute scale. In the calculation of energies the line position was defined as the line centre at half maximum. Lines that were not fully resolved by the spectrometer were separated graphically by the use of the known shape of a monoenergetic line. A large number of sufficiently isolated lines in the electron spectrum itself yielded, however, the necessary information about the line shapes in the various energy region.

A typical sample of the data taken during this investigation is displayed in Figs. 2, 3, 4, and 5. All parts of these figures were taken with an iron free  $\beta$ -ray spectrometer. Fig. 2 displays the K-conversion line from the intense 90 keV transition as well as the K-conversion lines of the 87, 91, 93, and 94 keV transitions. Fig. 3 shows a set of weak conversion lines which correspond to new  $\gamma$  rays not reported before. Figs. 4 and 5 show conversion lines from the energy range of  $\sim 110$  keV up to  $\sim 200$  keV.

The relative intensities of the conversion lines were obtained by measuring the areas under the corresponding conversion lines. In deducing the areas of partially resolved lines, we have found it convenient to subtract the background and  $\beta$  continuum rates. The line

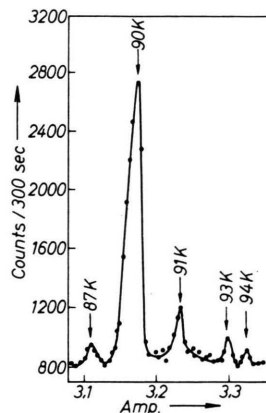


Fig. 2. The K-conversion lines of the 87, 90, 91, 93 and 94 keV transitions in  $^{147}\text{Pm}$ .

\*  $\beta$ -ray spectrometer type *B IIII-2* (Moscow 1957).

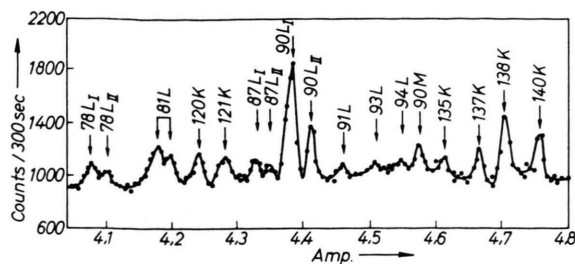


Fig. 3. Part of low energy conversion electron spectrum.

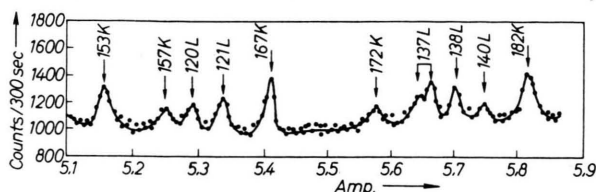


Fig. 4. Part of internal conversion lines of the 120, 121, 137, 138, 140, 153, 157, 167, 172 and 182 keV transitions.

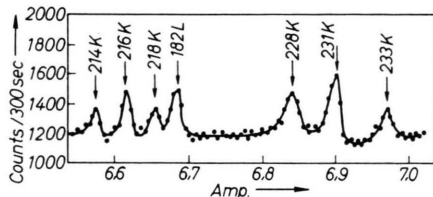


Fig. 5. The K-conversion lines of the 214, 216, 218, 228, 231 and 233 keV transitions.

shapes determined from clearly resolved lines of comparable energy and appropriate to the conversion shells in question are fitted to the data in this form. All closely spaced lines, except K lines, were assumed to have the same shape. This shape narrows quite gradually with increasing momentum, the contribution from energy degradation being less serious at high energies. For weaker lines the intensity was simply assumed to be proportional to the height compared with that of a neighbouring line of measured area. The conversion electron intensity results were corrected for the absorption in the mica counter window, in addition to the necessary corrections for the decay. The intensity errors assigned may be considered to represent standard deviations. They were calculated by combining in quadrature the standard deviations resulting from arithmetic procedures multiplied by a factor of 1.5 to take account of the non-statistical background uncertainty, together with the fixed figure of 2% which takes into account lack of reproducibility. The small errors assigned to some of the weak lines result from an intensive study of this particular portion of the spectrum.

Accurate conversion intensities, K/L- and L-subshell ratios of most of the transitions were determined. The experimental results were compared with the theoretical values for conversion coefficients.

## 2. Experimental Results

The energies, intensities and assignments of the conversion lines observed in this work are summarized in Table 1. The energies of the conversion lines are believed to have absolute uncertainties of  $\sim 0.2$  to  $0.3\%$ , this uncertainty resulting from: 1) a possible calibration error of one part in  $10^4$  in momentum arising from source position and degaussing uncertainties, 2) uncertainty in top line – centre position for these lines and 3) a possible error in the source thickness.

The transition energies and atomic shell assignments for the observed conversion lines were deduced using the tabulated<sup>11</sup> binding energies. Figs. 6 and 7 show the conversion spectrum of the 190.11, 198.23, 205.52, 208.28, 210.08, 214.54, 215.86, 217.92, 227.87, 239.82, 260.20, and 262.79 keV transitions which are revealed through their K- and L-shell conversion lines. Rather complex and weak conversion electron spectra due to  $\gamma$  rays of energies 190–326 keV have appeared for the first time in our measurements, see Fig. 8. Only a 320 keV transition had been observed previously, however, the high resolution adapted revealed instead three  $\gamma$  rays of energies 318.90, 322.43 and 326.24 keV. Also, as indicated in Fig. 9, some of the lines can be interpreted as K-conversion lines of transitions in the proposed level scheme. The good agreement between the transition energies, calculated from the level scheme and from the conversion lines, gives in some cases rather strong support to the interpretation of these lines as emitted in the decay of  $^{147}\text{Nd}$ . Moreover, in the conversion spectrum of  $^{147}\text{Nd}$  new peaks of 450(K), 460(K), 542(K) as well as 552(K) were found. The relative intensities and the assignments of the peaks are shown in Fig. 10. No  $\gamma$  rays of energy higher than 533 keV could be found by the scintillation technique except the 690 keV transition. The presence of weak  $\gamma$  rays in this region would be difficult to detect. From the sum coincidence technique undertaken by SASTRY et al.<sup>7</sup> a  $\gamma$  ray of energy  $723 \pm 7$  keV was observed and could be fitted in the level scheme. In our present investigations together with the prominent peaks due to previously reported  $\gamma$  rays, above 533 keV, there are a number of weak peaks in evidence. K-conversion electrons of new  $\gamma$  rays of energies 633, 643 and 724 keV were detected, Fig. 11.

<sup>11</sup> R. D. HILL, Beta and Gamma-ray Spectroscopy, edited by K. SIEGBAHN, North Holland Publ. Co., Amsterdam 1955.

Transition energy (keV)	Conversion shell	Experimental conversion coefficient	Theoretical conversion coefficient							Multipolarity	
			E1	E2	E3	E4	M1	M2	M3		M4
77.61 ± 0.03	L <sub>I</sub> /L <sub>II</sub>	2.00 ± 0.15	4.490	0.177	0.020	0.014	12.069	7.941	6.435	4.737	M1 + E2
81.30 ± 0.02	L <sub>I</sub> + L <sub>II</sub> /L <sub>III</sub>	1.06 ± 0.08	4.345	1.081	0.993	0.871	67.708	5.055	1.003	0.451	E2
87.64 ± 0.05	K/L	1.07 ± 0.09	6.414	1.057	0.1437	0.024	6.842	3.613	1.162	0.340	E2
90.76 ± 0.04	K	1.81 ± 0.20	0.295	1.53	6.2	23.7	1.85	17	100	540	M1 + E2
91.34 ± 0.05	K/L	6.92 ± 0.34	6.614	1.093	0.153	0.027	7.301	3.917	1.330	0.407	M1
93.06 ± 0.06	K/L	7.41 ± 0.32	6.713	1.087	0.151	0.028	7.214	3.874	1.271	0.383	M1 + E2
93.06 ± 0.06	K/L	5.21 ± 0.26	6.683	1.138	0.160	0.030	7.347	3.896	1.273	0.408	M1 + E2
94.31 ± 0.06	K/L	3.56 ± 0.12	6.700	1.240	0.177	0.032	7.124	3.820	1.349	0.356	M1 + E2
120.04 ± 0.08	K	0.68 ± 0.07	0.137	0.710	2.95	11.7	0.76	5.8	31	165	E2
121.32 ± 0.11	K/L	1.88 ± 0.14	6.667	1.978	0.362	0.093	6.638	4.345	1.881	0.752	E2
134.82 ± 0.09	K/L	1.91 ± 0.20	6.891	1.983	0.410	0.097	7.143	4.615	2.042	0.871	E2
136.89 ± 0.12	K/L	1.87 ± 0.17	6.711	1.975	0.455	0.129	6.996	4.767	2.328	0.925	E2
136.89 ± 0.12	K/L	6.94 ± 0.39	6.776	2.153	0.510	0.147	7.200	4.545	2.395	1.073	M1
138.26 ± 0.10	K/L	6.82 ± 0.42	6.963	2.146	0.525	0.145	7.072	4.663	2.346	1.021	M1
140.09 ± 0.08	K/L	1.91 ± 0.16	6.820	2.287	0.558	0.158	7.033	4.888	2.358	1.005	E2
153.22 ± 0.14	K/L	5.97 ± 0.47	6.890	2.540	0.6890	0.224	6.709	4.962	2.600	1.277	M1 + E2
157.04 ± 0.12	K/L	6.58 ± 0.32	6.694	2.768	0.728	0.221	6.757	4.691	2.564	1.313	M1
166.94 ± 0.09	K/L	2.35 ± 0.18	6.699	2.793	0.708	0.237	6.588	5.080	2.440	1.434	M3
172.12 ± 0.10	K/L	5.67 ± 0.31	6.745	2.975	0.744	0.299	7.192	5.132	2.723	1.516	M1 + E2
182.10 ± 0.15	K/L	6.54 ± 0.42	6.769	3.145	0.924	0.356	6.995	5.028	2.721	1.475	M1
190.11 ± 0.10	K/L	3.61 ± 0.23	6.870	3.358	1.036	0.419	7.529	5.643	3.210	1.667	E2
198.23 ± 0.12	K/L	3.37 ± 0.17	7.377	4.302	1.107	0.476	7.570	6.277	3.481	1.923	M3
205.32 ± 0.20	K/L	7.04 ± 0.65	6.926	3.418	1.115	0.476	7.306	5.666	3.257	1.872	M1
208.28 ± 0.16	K/L	7.00 ± 0.69	7.275	3.564	1.179	0.480	7.485	6.171	3.532	1.975	M1
210.08 ± 0.19	K/L	3.09 ± 0.27	6.829	3.472	1.166	0.479	7.281	5.949	3.448	1.933	E2
214.54 ± 0.20	K/L	6.12 ± 0.59	6.985	3.598	1.235	0.494	7.593	6.143	3.638	2.132	M1 + E2
215.86 ± 0.22	K/L	5.44 ± 0.52	6.822	3.528	1.224	0.489	7.363	5.517	3.549	2.077	M1 + E2
217.92 ± 0.09	K/L	4.98 ± 0.47	6.568	3.520	1.270	0.513	7.281	5.952	3.539	2.027	M1 + E2
227.87 ± 0.14	K/L	6.93 ± 0.41	6.768	3.817	1.431	0.587	7.384	6.250	3.599	2.105	M1 + E2
230.93 ± 0.11	K/L	3.34 ± 0.22	6.831	3.665	1.422	0.581	7.327	5.983	3.644	2.152	M3
233.22 ± 0.19	K/L	6.85 ± 0.47	6.725	3.644	1.364	0.569	7.172	5.832	3.460	2.066	M1
239.82 ± 0.21	K/L	0.90 ± 0.08	7.043	3.889	1.508	0.645	7.678	6.445	3.976	2.548	E4
260.20 ± 0.15	K/L	4.99 ± 0.32	7.004	4.101	1.720	0.791	7.738	6.137	4.015	2.716	M1 + E2
262.79 ± 0.13	K/L	7.48 ± 0.68	6.815	3.987	2.071	0.759	7.677	6.145	3.904	2.603	M1
273.25 ± 0.18	K/L	3.87 ± 0.22	6.892	4.161	1.918	0.867	7.902	6.151	4.503	2.627	E2
277.21 ± 0.23	K/L	7.21 ± 0.39	6.983	4.264	1.913	0.909	7.537	6.368	4.221	2.647	M1
278.75 ± 0.24	K/L	7.14 ± 0.46	6.938	4.173	1.856	0.872	7.544	6.401	4.241	2.659	M1 + E2
282.71 ± 0.21	K/L	6.89 ± 0.62	7.064	4.250	1.862	0.880	7.605	6.250	4.178	2.819	M1
289.64 ± 0.25	K/L	7.34 ± 0.58	6.993	4.255	1.960	1.012	7.712	6.093	3.992	3.059	M1
292.95 ± 0.21	K/L	4.00 ± 0.29	6.691	4.174	1.906	0.986	7.728	6.128	4.023	3.071	E2
302.47 ± 0.29	K/L	6.35 ± 0.58	7.151	4.396	2.102	1.016	7.218	6.027	4.141	2.949	M1 + E2
306.89 ± 0.24	K/L	5.21 ± 0.45	7.165	4.602	2.139	1.060	7.168	5.924	4.390	2.976	M1 + E2
308.91 ± 0.30	K/L	6.84 ± 0.52	6.875	4.343	2.070	1.048	7.169	5.938	4.412	2.991	M1 + E2
318.90 ± 0.22	K	0.055 ± 0.006	0.0102	0.034	0.107	0.345	0.057	0.225	0.84	2.45	M1
322.43 ± 0.28	K/L	7.20 ± 0.32	6.809	4.277	2.162	1.078	7.287	5.859	4.492	2.849	M1 + E2
326.24 ± 0.30	K/L	6.87 ± 0.43	6.798	4.258	2.244	1.106	7.117	5.864	4.594	2.857	M1
		7.23 ± 0.75	6.735	4.204	2.227	1.067	7.136	5.889	4.629	2.868	M1

Transition energy (keV)	Conversion shell	Experimental conversion coefficient	Theoretical conversion coefficient								Multipolarity
			E1	E2	E3	E4	M1	M2	M3	M4	
343.81 $\pm$ 0.26	K/L	6.62 $\pm$ 0.61	7.131	4.524	2.478	1.244	6.763	6.000	4.380	2.960	M1
349.97 $\pm$ 0.31	K/L	5.40 $\pm$ 0.48	7.404	4.621	2.508	1.275	7.084	5.957	4.746	3.193	M1 + E2
369.65 $\pm$ 0.29	K/L	6.38 $\pm$ 0.44	7.171	4.925	2.669	1.359	7.311	6.071	4.718	4.035	M1 + E2
371.50 $\pm$ 0.24	K/L	7.44 $\pm$ 0.53	7.151	4.839	2.622	1.345	7.311	6.071	4.718	4.035	M1
397.84 $\pm$ 0.25	K/L	7.92 $\pm$ 0.41	7.641	5.220	3.028	1.615	7.773	6.749	5.465	4.167	M1
400.32 $\pm$ 0.31	K/L	7.61 $\pm$ 0.37	7.449	5.137	2.944	1.593	7.530	6.468	5.170	3.913	M1
405.12 $\pm$ 0.37	K/L	7.33 $\pm$ 0.61	7.531	5.201	2.914	1.580	7.615	6.297	5.288	4.096	M1
413.10 $\pm$ 0.32	K	0.024 $\pm$ 0.004	0.00579	0.017	0.0465	0.128	0.028	0.1	0.31	0.94	M1 + E2
	K/L	6.73 $\pm$ 0.33	7.404	5.280	2.981	1.718	7.212	6.277	5.099	4.017	
442.64 $\pm$ 0.33	K/L	5.42 $\pm$ 0.21	7.432	5.263	3.140	1.833	7.614	6.788	5.724	4.644	E2
450.63 $\pm$ 0.41	K/L	4.95 $\pm$ 0.57	7.571	5.480	3.348	1.859	7.751	6.775	5.679	5.752	E2
459.50 $\pm$ 0.46	K/L	4.88 $\pm$ 0.24	7.603	5.522	3.505	2.000	7.373	6.475	5.707	4.240	E2
491.02 $\pm$ 0.39	K/L	7.30 $\pm$ 0.41	7.634	5.691	3.590	2.315	7.235	6.546	6.076	4.831	M1
508.23 $\pm$ 0.42	K/L	6.51 $\pm$ 0.32	7.757	5.581	3.582	2.210	7.052	6.301	5.611	4.128	M1 + E2
533.41 $\pm$ 0.29	K	0.010 $\pm$ 0.001	0.0033	0.0084	0.0215	0.051	0.0145	0.046	0.125	0.325	E2
	K/L	5.65 $\pm$ 0.24	7.746	5.676	3.952	2.550	7.084	6.623	5.855	4.656	
541.93 $\pm$ 0.34	K/L	6.99 $\pm$ 0.48	7.768	5.765	4.008	2.553	7.312	6.897	6.076	4.874	M1 + E2
552.23 $\pm$ 0.49	K/L	6.83 $\pm$ 0.65	7.417	5.495	3.900	2.514	7.235	6.636	6.082	4.951	M1
599.20 $\pm$ 0.36	K	0.0012 $\pm$ 0.0003	0.0025	0.00639	0.0158	0.0365	0.0108	0.032	0.08	0.215	
	K/L	7.23 $\pm$ 0.67	7.452	5.836	4.270	2.874	7.143	6.524	5.797	4.886	
633.13 $\pm$ 0.52	K/L	7.34 $\pm$ 0.53	7.772	6.313	4.686	3.333	7.573	6.979	6.696	5.255	M1
642.82 $\pm$ 0.60	K/L	6.44 $\pm$ 0.46	7.427	6.034	4.410	3.118	7.573	6.979	6.696	5.255	M3
690.10 $\pm$ 0.42	K	0.0065 $\pm$ 0.0007	0.00182	0.0046	0.0105	0.0235	0.0078	0.022	0.05	0.12	M1 + E2
	K/L	6.89 $\pm$ 0.51	7.444	6.301	4.688	3.497	7.239	6.647	5.734	5.298	
724.01 $\pm$ 0.53	K/L	7.24 $\pm$ 0.47	7.240	6.042	4.721	3.741	7.089	6.502	5.726	5.526	M1
763.12 $\pm$ 0.60	K/L	7.02 $\pm$ 0.54	7.514	6.433	5.085	4.089	7.166	6.662	6.091	5.231	M1

Table 1. Energies, conversion coefficients and multiplicities of transitions measured in this investigation.

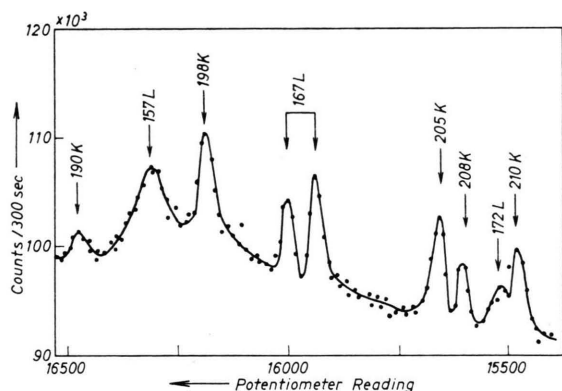


Fig. 6. Internal conversion spectrum of 190 K, 198 K, 167 L, 205 K, 208 K, 172 L and 210 K lines.

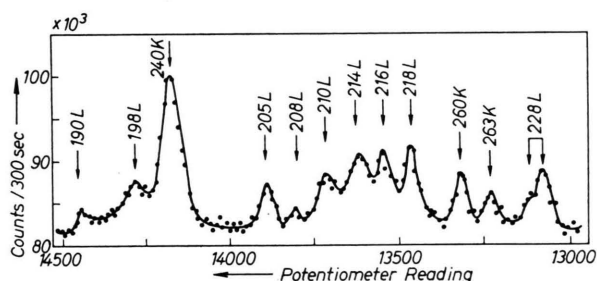


Fig. 7. The L- and K-conversion lines of  $\gamma$  rays of energy about 190–263 keV.

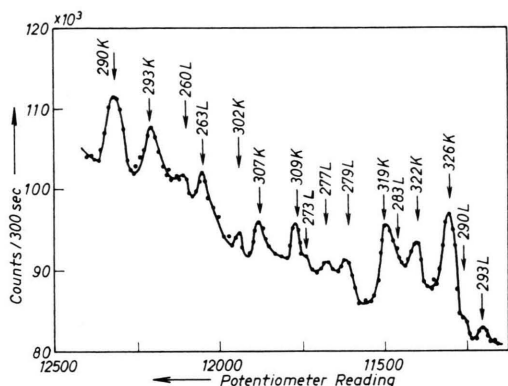


Fig. 8. The K-conversion lines of the 290, 293, 302, 307, 309, 319, 322 and 326 keV transitions together with the L-conversion lines of the 260, 263, 273, 277, 279, 283, 290 and 293 keV transitions.

The transition energies determined in the present investigation are summarized in Table 1. There is excellent agreement between the  $\gamma$  transitions found by the present authors and those of SASTRY et al.<sup>7</sup>. A total of 66  $\gamma$  transitions have been found in the decay of  $^{147}\text{Nd}$ .

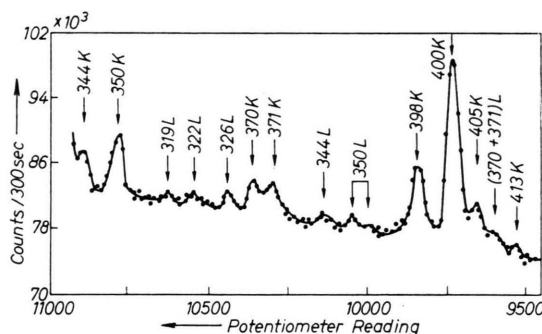


Fig. 9. Part of internal conversion spectrum shows mainly the K lines of the 344, 370, 371, 398, 400, 405 and 413 keV transitions in  $^{147}\text{Pm}$ .

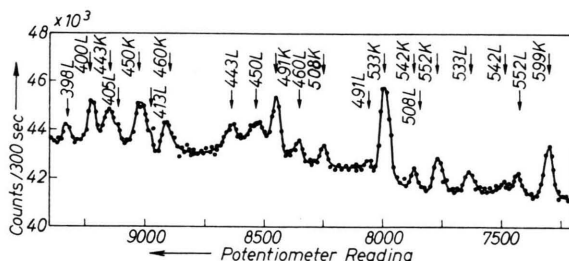


Fig. 10. The L- and K-conversion lines of  $\gamma$  rays of energy 398–599 keV.

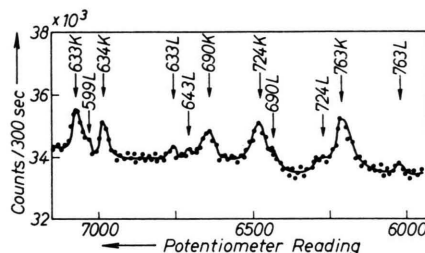


Fig. 11. The high energy part of internal conversion spectrum from the decay of  $^{147}\text{Nd}$ .

## 2.1 Multipolarities

The present conversion electron spectrum study which yields ratios for conversion electron intensities in different shells and subshells should possibly give information about the multipole orders of the transitions. The multipolarities of most transitions are based on comparison of measured K/L- and L-subshell ratios with the corresponding theoretical ratios derived by interpolation from the K- and L-shell conversion coefficients calculated by SLIV and BAND<sup>12</sup>, and also from comparison of the absolute conversion coefficients with the theoretical ones. By means

<sup>12</sup> L. A. SLIV and I. M. BAND, Tables of Internal Conversion Coefficients, Izv. Akad. Nauk SSR, Moscow—Leningrad [1958].

of the photon intensities<sup>13</sup> and the conversion electron data of some transitions, we have calculated the absolute conversion coefficients which are presented in Table 1. Normalization between the two series of data is obtained by assuming that the 533 keV transition is a pure E2 transition with K-conversion coefficient equal to 0.0084.

The mixing ratio  $\delta^2$  ( $\delta^2 = E2/M1$ ), has been determined for the 77.61, 90.76, 93.06, 94.31, 172.12, 260.20, 278.75, 322.43, 413.10, 508.23, 552.23 and 690.10 keV transitions either from the absolute conversion coefficients or from the conversion electron ratios, see Table 2. The results obtained were compared with previous results determined from directional correlation measurements.

Transition energy (keV)	Mixing ratio $\delta^2 = E2/M1$	Calculated from
77.61 $\pm$ 0.03	0.145 $\pm$ 0.019	L <sub>1</sub> /L <sub>11</sub> ratio
90.76 $\pm$ 0.04	0.076 $\pm$ 0.008	$\alpha_K$ and K/L ratio
93.06 $\pm$ 0.06	0.099 $\pm$ 0.010	K/L ratio
94.31 $\pm$ 0.06	0.314 $\pm$ 0.041	K/L ratio
172.12 $\pm$ 0.10	0.287 $\pm$ 0.032	K/L ratio
260.20 $\pm$ 0.15	2.44 $\pm$ 0.25	K/L ratio
278.75 $\pm$ 0.24	0.115 $\pm$ 0.014	K/L ratio
322.43 $\pm$ 0.28	0.095 $\pm$ 0.011	K/L ratio
413.10 $\pm$ 0.32	0.520 $\pm$ 0.063	$\alpha_K$ and K/L ratio
508.23 $\pm$ 0.42	0.800 $\pm$ 0.080	K/L ratio
552.23 $\pm$ 0.49	0.424 $\pm$ 0.045	K/L ratio
690.10 $\pm$ 0.42	0.775 $\pm$ 0.082	$\alpha_K$ and K/L ratio

Table 2. Experimental values of the mixing ratio of some transitions in <sup>147</sup>Pm.

### 3. Decay Scheme of <sup>147</sup>Nd

#### 3.1 Energy levels of <sup>147</sup>Pm

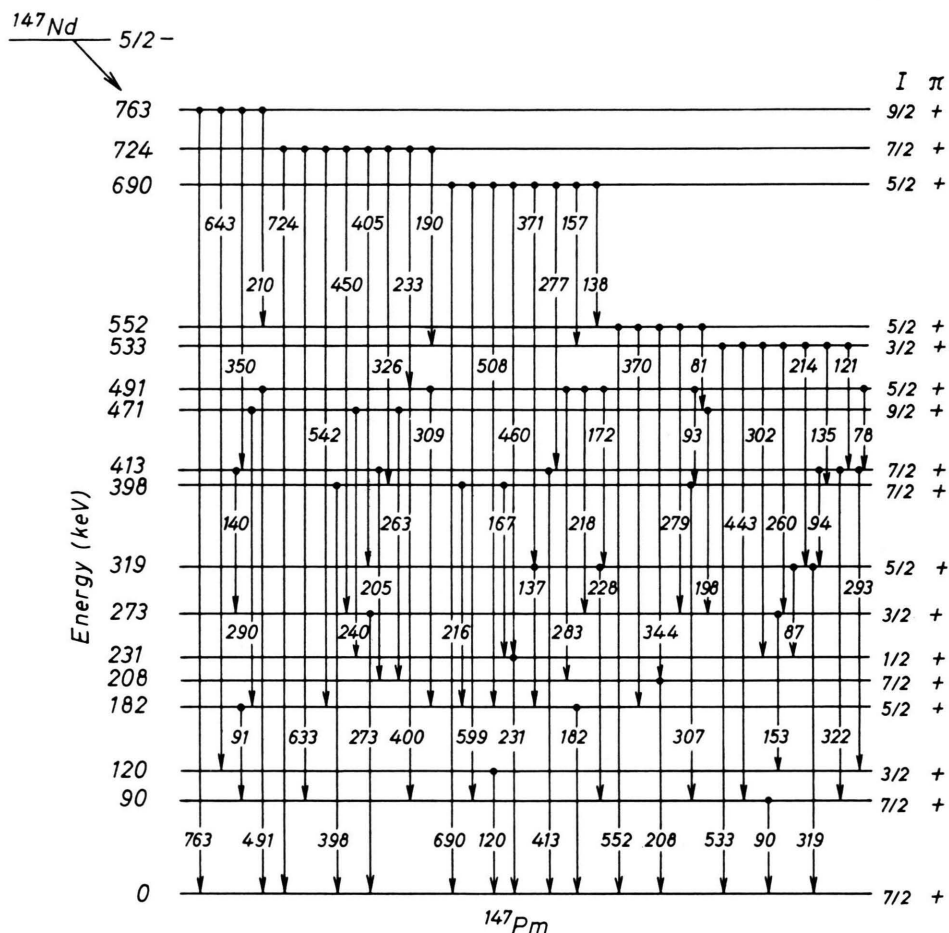
In constructing a decay scheme from the observed transitions, consideration was first given to the energy levels suggested by SASTRY et al.<sup>7</sup>. Their coincidence results unambiguously confirm seven excited states at 91, 182, 413, 491, 533, 690, and 723 keV, which accommodate 17  $\gamma$  transitions with a very good energy fitting, as shown in Fig. 1 a. A search for further excited states was made by investigating the numerical relationships between the transition energies. As a first step, relationships of the type  $E_1 + E_2 = E_3$  were studied. All possible energy sums of pairs of transitions in Table 1 were calculated and compared with the energy of a third transition.

Although in the present investigation the accuracies of the transition energies are rather good, the number of random cases was found to be considerable for some types of configurations. This calculation showed that in many cases the sum of the energies of two transitions equalled the energy of a third transition within the limits of error. It is therefore demonstrated that the majority of the sum relationships are likely to correspond to true cascade cross-over combinations. This calculation gives strong support for further energy levels. Transitions previously located in the decay scheme were discounted in this estimate. In an attempt to find further energy levels, a search was made for levels supported by a minimum of two transitions which connected with confirmed levels discussed above. The decay scheme deduced from the data is shown in Fig. 12. The existence of the 120, 182, 231 and 273 keV levels has been confirmed in our investigation, which is supported by the appearance of direct ground state transitions, as shown in Figs. 1 b and 12. The 319 and 398 keV levels proposed by RUTLEDGE et al.<sup>4</sup> evidently appeared in our present decay scheme and are followed by the 318.90 and 397.84 keV transitions to the ground states. These transitions have also been observed in the conversion electron measurement reported by RUTLEDGE et al.<sup>4</sup>. The 413, 491, 533, 690, and 723 keV levels are consistent with the measurements of SASTRY et al.<sup>7</sup>, however the modes of decay are slightly different due to the appearance of weak transitions which could not be detected before. The existence of three more new levels at 471, 552 and 763 keV is proposed to accommodate the  $\gamma$  transitions found.

#### 3.2 Spin Assignment

Spin and parity information was derived from the multiplicities and the log  $ft$  values in the following manner. Since knowledge of the multipolarity of a ground state transition immediately leads to an assignment of spin and parity, transitions of this type were first studied. The spin and parity of the ground state of <sup>147</sup>Nd has been known to be 5/2<sup>-</sup> from ABRAHAM's investigation<sup>8</sup>. The ground state of <sup>147</sup>Pm, as was discussed<sup>7</sup>, can be assigned 7/2<sup>+</sup>. All the  $\beta$  transitions from the ground state of <sup>147</sup>Nd and feeding the excited states of <sup>147</sup>Pm have been classified as first-forbidden with a spin change of zero or one and with change of parity<sup>3, 4</sup>. On these basis the spin and parity assignments of the excited states are suggested.

<sup>13</sup> Nuclear Data Sheets, National Academy of Sciences, Washington D. C. 1961.

Fig. 12. Proposed decay scheme of  $^{147}\text{Nd}$ .

**Levels below 400 keV:** The spin and parity  $7/2+$  assignment for the first excited level 90 keV, is compatible with the observed 90.76 keV  $M1 + E2$  transition to the ground state. The 90.76 keV transition was identified by observing the K,  $L_1 + L_{11}$ - and  $L_{11}$ -conversion electrons. The K/L ratio requires a small E2 admixture of about 7% which is in satisfactory agreement with the angular correlation measurement<sup>10</sup>. Coincidence experiments<sup>7</sup> have shown that the 90 keV level is fed by  $\gamma$  rays of 91, 332, 400, 442 and 599 keV. In addition, the present measurements have proposed the existence of weak feeding by  $\gamma$  rays of 227.87, 306.89 and 633.13 keV.

The 120 keV level was firstly suggested by RUTLEDGE et al.<sup>4</sup>, however, SASTRY et al.<sup>7</sup> excluded its existence and placed the 120 keV transition between the 533 and 413 keV levels. The 120 keV level is again proposed in our constructed decay scheme for

$^{147}\text{Pm}$ , where it is de-excited to the ground state by the 120.04 keV transition. A new  $\gamma$  ray of energy 121.32 keV was observed in our conversion electron spectrum and it is an energetically perfect fit between the 533 and 413 keV levels. There are two transitions 153.22 and 642.82 keV feeding the 120 keV level decaying from the 273 and 673 keV levels respectively. From the relative intensities of the conversion electrons, and the absolute K-conversion coefficient it was confirmed that the 120 keV is pure E2 transition which suggests the spin and parity of  $3/2+$  or  $11/2+$ . The  $3/2+$  assignment is more favourable, since it is compatible with the multipolarities of the transitions feeding this level.

GUNYE et al.<sup>6</sup> were not in favour of introducing a level at 182 keV and they put an upper limit of less than one percent for the intensity of  $\beta$  transition to this level if it exists. SASTRY et al.<sup>7</sup> have shown

by the sum coincidences that there are cascades from the levels 690 and 533 keV to the 182 keV level. However, as pointed out already, these branching ratios are small. In addition the levels at 690 and 533 keV are themselves fed by  $\beta$  decay of  $^{147}\text{Nd}$  through 3.5 and 16%, respectively. The cascade transitions from 491 and 413 keV levels to the 182 keV level could not be inferred from coincidence investigation<sup>7</sup> because of the confusing background. Therefore, it was concluded<sup>7</sup> that the intensities of  $\gamma$  lines 508 (690  $\rightarrow$  182) and 351 (533  $\rightarrow$  182) keV must be small and it is likely that the earlier investigators missed these lines. Our present investigation gives new information on the 182 keV level since it shows cascades from the 724, 690, 552, 491, 471, 398 and 319 keV levels. All these transitions are weak. But the most striking feature is that the cascade from the strong 533 keV level is excluded in the proposed decay scheme. It is also necessary to assume that the  $\beta$  group feeding the 182 keV level, if any, must be very small. The mode of decay of the 182 keV level as inferred from the present studies and from the sum coincidence measurement<sup>7</sup>, is through a (90.76 + 91.36) keV cascade and a cross-over transition. For the energy level at 182 keV, three possible spin values  $3/2+$ ,  $5/2+$  or  $7/2+$  were suggested, though any definite conclusion regarding spin value, could not be drawn<sup>7</sup>. The multipolarities of the transition feeding and de-exciting this level favour spin and parity  $5/2+$ .

The level at 208 keV is proposed according to the appearance of  $\gamma$  rays of energy 208.28 keV in our measurements. The K- and L-conversion electrons of the 208.28 keV transition were observed for the first time in the internal conversion spectra from the decay of  $^{147}\text{Nd}$ . The multipolarity of the 208 keV is pure M1 as determined from the K/L-conversion ratio. Due to this assignment the spin and parity  $5/2+$ ,  $7/2+$  or  $9/2+$  are possible for the 208 keV level. The 208 keV level is fed by the 205.52, 262.79, 282.71 and 343.81 keV transitions. The determined multipolarity assignments for these transitions confirm the spin and parity  $7/2+$ .

On the basis of pure M3 transition between the 231 keV level and the ground state, the spin of the 231 keV level is probably  $1/2+$ . It was difficult to prove that the 231 keV transition is an M3 since the K/L ratio is equally the same for E2 and M3 character, see Table 1. However, the weak intensity of

the 231 keV  $\gamma$  ray is in agreement with the M3 assignment.

The E2 character of the 273.25 keV and the M1 character of the 318.90 keV transitions to the  $7/2+$  ground state suggest the spin and parity of the 273 and 319 keV levels as  $3/2+$  and  $5/2+$  respectively, considering the multipolarities of the transitions feeding and de-exciting them.

The 398 keV level is de-excited by a strong ground state transition. The conversion electron ratio K/L of the 397.84 keV  $\gamma$  ray agrees with the value for pure M1 transition. Consequently, the spin and parity of the 398 keV level is consistent with  $5/2+$ ,  $7/2+$  or  $9/2+$ . According to the pattern of transitions feeding this level and the pure E2 character of the 166.94 keV transition decaying from this level to the  $1/2+$  (231 keV) level, the  $5/2+$  and  $9/2+$  assignments are excluded.

*Levels above 413 keV:* The spin and parity could be estimated for the 413 keV level, since it is populated by an M1 + E2 transition (78 keV) from  $5/2+$  491 keV excited state, a pure M1 transition (277 keV) from  $5/2+$  690 keV excited state and the pure E2 transition (121 keV) from the  $3/2+$  533 keV excited state, and also since it is de-excited to the  $7/2+$  ground state by an M1 + E2 transition (413.10 keV) as proved from the conversion electrons ratio as well as from the absolute K-conversion coefficient, as illustrated in Table 1.  $7/2+$  assignment is proposed for the 413 keV level according to the conversion coefficients data, however,  $5/2+$  and  $9/2+$  could not be ruled out. This assignment is in agreement with  $7/2+$  determined from angular correlation experiments<sup>10</sup>.

A new level is suggested at 471 keV which is fed by 81.32 keV  $\gamma$  ray from the 552 keV excited level. The decay of the 471 keV level to the ground state is not observed. It is de-excited to the 182, 208, 231 and 273 keV levels by  $\gamma$  rays of energies, 289.64, 262.79, 239.82 and 198.23 keV respectively. This phenomenon is difficult to explain unless a  $\beta$  branch is feeding this level together with the 81.32 keV  $\gamma$  ray. The multipolarity assignments for these mentioned transitions make the spin and parity  $9/2+$  and the most convenient values for the 471 keV level.

The observed M1 multipolarity of the 491 keV ground state transition favours a spin and parity of  $5/2+$  for this level. A new 233.22 keV  $\gamma$  ray with M1 character was found feeding the 491 keV level.

The 533 keV level is fed mainly by a strong  $\beta$  transition from  $^{147}\text{Nd}$  and de-excited by strong  $\gamma$  rays of energies 533.41 and 442.64 keV. Additional weak  $\gamma$  rays, 302.47, 260.20, 214.54, 121.30 and 134.82 keV were also found de-exciting this level. On account of the sum energy relations, the 157.04 and 190.11 keV  $\gamma$  rays are feeding the 533 keV level. The conversion coefficients of the 533 keV  $\gamma$  ray proved that it has pure E2 character. By the K/L-conversion ratio alone the multipolarity could not be estimated, since a value of 5.65 for this ratio is compatible with either E2 character ( $K/L=5.67$ ) or M3 character ( $K/L=5.85$ ). However, the absolute K-conversion coefficient could differentiate between the two multiplicities. The present results are in good agreement with the previous conversion results<sup>14</sup>. Therefore a  $3/2+$  assignment is proposed for the 533 keV level.

A level at 552 keV is proposed according to the energy sums of the (370+182), (279+273) and (344+208) keV together with the appearance of  $\gamma$  ray with energy of 552.23 keV. This level is fed by a  $\gamma$  ray of energy 138.26 keV de-exciting the 690 keV level and a  $\gamma$  ray of energy 210.08 keV de-exciting the 763 keV level. The spin and parity  $5/2+$  are assumed due to the multiplicities of the feeding and de-exciting transitions and also due to the indicated M1 + E2 character of the 552.23 keV transition to the ground state.

The 690 keV level is de-excited to the ground state by the 690.10 keV transition. No  $\gamma$  rays were observed feeding the 690 keV level and it is presumably fed by a  $\beta$  transition. The measured K-internal conversion line intensity and  $\gamma$ -ray intensity of the 690 keV  $\gamma$  ray gave the conversion coefficient  $\alpha_K = 0.0065 \pm 0.0007$ . This value agrees with the theoretical coefficient for M1 with an admixture of quadrupole character, see Table 2. Conversion lines of the 690 keV transition were not previously observed, as a consequence the multipolarity could not be assigned. The conversion coefficients data suggest spin and parity either  $5/2+$ ,  $7/2+$  or  $9/2+$ . The E2 character of the 459.50 keV transition, placed between the 690 and 231 keV levels, assigned  $5/2+$  for the 690 keV level which is in agreement with the angular correlation results<sup>10</sup>.

In the sum coincidence spectrum<sup>7</sup> for 723 keV, a sum peak at 723 keV alone was obtained with no

other peaks for the possible cascades. As suggested by GUNYE et al.<sup>6</sup>, the 723 keV excited level decays by a cascade (410+310), however SASTRY et al.<sup>7</sup> concluded that the 723 keV level exists but its decay is mainly through a cross-over transition to the ground state. From our internal conversion measurements we found both a direct transition to the ground state and different cascades, as shown in Fig. 12. It may be noted that intensities of the  $\gamma$ -ray cascades are small, in addition, the high energy level at 724 keV is fed by a percentage of  $\beta$  transition from  $^{147}\text{Nd}$  or probably low  $\gamma$ -ray energy de-exciting the higher excited level at 763 keV. Due to the M1 character of the 724.01 keV transition together with the other multiplicities of the  $\gamma$  transitions de-exciting the 724 keV level, a  $7/2+$  assignment is suggested.

The presence of the 763 keV excited level in  $^{147}\text{Pm}$  solved the location of the 210.08, 349.97, 642.82 and 763.12 keV transitions in the decay of  $^{147}\text{Nd}$ . The spin and parity of the 763 keV level are supposed to be  $9/2+$ .

#### 4. Discussion

The level structure of  $^{147}\text{Pm}$  resulting from the present work differs from the schemes proposed by earlier investigators<sup>4,7</sup>. The principal  $\gamma$  transitions found in reference<sup>7</sup> have been identified here and the different cascades have been confirmed. However, the present results differ in the energies and positions of some of the other  $\gamma$  transitions. By means of intensity data and the directional correlation measurement<sup>10</sup>, it has been possible to limit the probable spin assignments for most of the levels. More information is needed in order to interpret the low-lying level structure of  $^{147}\text{Pm}$ . Therefore some speculation based on the present results may be useful.

The  $^{147}\text{Pm}$  nucleus has 61 protons and 86 neutrons. It lies just below the region of stable deformed nuclei. Empirically the transition to deformed shape is observed to take place for neutron number between 88 and 90. The NILSSON model has been successful in predicting the level structure in the deformed region<sup>15</sup>. If one attempts to interpret the present level structure in these terms, one is forced to choose the  $(7/2+, 404)$  orbital for the ground

<sup>14</sup> H.W. WRIGHT, E. I. WYATT, S. A. REYNOLDS, W. S. LYON, and T. H. HANDLEY, Nucl. Sci. Eng. **2**, 427 [1957].

<sup>15</sup> B. R. MOTTELSON and S. G. NILSSON, Kgl. Danske Videnskab. Selskab, Mat. Fys. Skrifter **1**, No. 8 [1959].

state of  $^{147}\text{Pm}$ . However, in order to consider this choice a small deformation parameter is required. This is not reasonable compared to other deformation parameters in this region and one concludes that the NILSSON approach is not applicable here. Even if the additional freedom of non-axially symmetric shapes is allowed in accordance with the calculations of HECHT and SATCHLER<sup>16</sup>, it is not possible to account for the spins and parities found in the present work. Finally, we may compare the level structure with the calculations of KISSLINGER and SORESENSEN<sup>17</sup>, in which the spectra of spherical nuclei with residual forces have been predicted. The main

assumption of this theory is that the low-lying states of spherical nuclei can be treated in terms of two basic excitations, quasi-particles and phonons. For the most part these are treated as separate modes of motion. For even-even nuclei the lowest excitations are the phonons, and only these are treated in detail. For the odd-mass nuclei both of these modes of excitations are low in energy and are considered as well as their interactions. However, these calculations are not fully successful in predicting  $^{147}\text{Pm}$  structure especially for the low-lying levels. These facts have been observed in the neighbouring  $^{149}\text{Pm}$  nucleus.

<sup>16</sup> K. T. HECHT and G. R. SATCHLER, Nucl. Phys. **32**, 286 [1962].

<sup>17</sup> L. S. KISSLINGER and R. A. SORESENSEN, Rev. Mod. Phys. **35**, 853 [1963].

## Composition Dependence of the Thermal Diffusion Factor in Binary Gas Mixtures

B. P. MATHUR \* and S. C. SAXENA \*\*

Department of Physics, University of Rajasthan, Jaipur, India

(Z. Naturforschg. **22 a**, 164—169 [1967] ; received 15 October 1966)

The thermal diffusion factor,  $\alpha_T$ , for the gas systems He—Ar, He—Ne, Ne—Kr and Ne—Xe is measured as a function of composition in a glass two bulb apparatus, operating with its hot and cold bulbs at 373.9° and 273.3 °K respectively. Gas samples are analysed with a sensitive and specially designed differential thermal conductivity analyser. The  $\alpha_T$  data are compared with similar values of other workers and a smooth set is recommended. The data are further compared with the predictions of rigorous theory in conjunction with realistic intermolecular potentials. An approximate prediction of the theory concerning the composition dependence of  $\alpha_T$  has been checked.

Many efforts have been made to measure the thermal diffusion factor  $\alpha_T$ , for binary mixtures of gases and these are summarized by GREW and IBBS<sup>1</sup>, and MASON, MUNN and SMITH<sup>2</sup>. SAXENA and MATHUR<sup>3-5</sup> have interpreted some of these data in a series of three articles. During these studies a need for a number of specialised investigations came into light. The present work is polarized towards such deficiencies and particularly deals with the composition dependence of  $\alpha_T$ . The mixtures of noble gases have been investigated in view of the fact that

the CHAPMAN—ENSKOG theory strictly applies only to such monatomic spherically symmetric molecules. The specific binary systems covered are He—Ar, He—Ne, Ne—Kr and Ne—Xe.

### Experimental Procedure and Results

For our measurements the known two bulb thermal diffusion apparatus is used with the volumes  $V_1=193.5$  cc and  $V_2=30.3$  cc. The two volumes can be separated by a stopcock and the two bulbs

\* Department of Physics, Kurukshetra University, Kurukshetra, India.

\*\* Thermophysical Properties Research Center, Purdue University, Lafayette, Indiana, U.S.A.

<sup>1</sup> K. E. GREW and T. L. IBBS, Thermal Diffusion in Gases, Cambridge University Press, New York 1952.

<sup>2</sup> E. A. MASON, R. J. MUNN, and F. J. SMITH, Advan. in Atomic and Molecular Physics (Ed. D. R. BATES and I. ESTERMANN), Academic Press Inc., New York 1965.

<sup>3</sup> S. C. SAXENA and B. P. MATHUR, Rev. Mod. Phys. **37**, 316 [1965].

<sup>4</sup> S. C. SAXENA and B. P. MATHUR, Rev. Mod. Phys. **38**, 380 [1966].

<sup>5</sup> S. C. SAXENA and B. P. MATHUR, J. Sci. Indust. Res. India **25**, 54 [1966].